

EFFECTS OF CHILLS ON THE SOLIDIFICATION PATTERN OF AN AXIAL STEEL CAST IMPELLER

Received – Priljeno: 2013-06-04
Accepted – Prihvaćeno: 2014-10-30
Preliminary Note – Prethodno priopćenje

This paper presents three-dimensional simulation of transient conduction heat transfer within an axial impeller (AISI 1016), two different sizes of chills (AISI 1016), core (green sand) and mold (green sand) by using Ansys CFX. Specific heat, density and thermal conductivity of AISI 1016 steel, mold and Core materials are considered as functions of temperatures

Key word: steel casting; solidification; impeller; finite volume modeling; heat transfer of casting

INTRODUCTION

It is a necessity to feed the liquid metal from the riser(s) to all geometric locations from the beginning to the end of the solidification. Although large amount of data are available to define feeding distances, all data are generated for the simple shapes. Thus, for complex cast geometries, numerical analysis should be employed to know the solidification pattern and to modify it by special applications such as the use of chills.

The feeding distances of risers are increased by using chills. The difficulties in defining feeding distances of risers in complex cast geometries become harder in cases that foundry engineers intent to use chills for which no quantitative data are available.

The most effective way to understand how a chill modifies the solidification pattern and feeding distance is to use numerical methods by adding chills as new domains to the models analyzed.

The accuracy of numerical techniques depends on the use of correct thermo-physical properties of metals and mold at elevated temperatures that were studied by several researchers [1-8].

The object of this article is to analyze the change in the solidification pattern of an axial impeller by the use of chills, both made of AISI 1016 steel, poured into green sand. This analyze is carried out by using a commercial Finite Volume Package, Ansys CFX.

The pouring temperature was set as 1 973 K in order to ensure the proper flow through thin blades. The density, specific heat, thermal conductivity of AISI 1016 steel, chills, mold and core sand were considered as temperature dependent.

THERMAL GOVERNING EQUATION

It is identical to the transient energy equation given in the following formula [9].

$$\nabla(k(T)\nabla T) = \frac{\partial}{\partial t} [\rho(T)C_p(T)T] \quad (1)$$

Where

ρ is the density.

k is thermal conductivity. and

C_p is specific heat including latent heat of solidification.

THERMOPHYSICAL PROPERTIES OF AISI 1016 STEEL AND GREEN SAND

Thermo-physical data of AISI 1016 steel and machine molded green sand are presented in Table 1 and Table 2 respectively.

Table 1 Thermo-physical properties of AISI 1016 steel [3]

T /K	AISI 1016		
	ρ	C_p	k
	kg/m ³	J/kg K	W/m K
298	7 964	446	14,51
473	7 890	487	16,85
673	7 804	522	19,54
873	7 717	556	22,24
1 073	7 631	590	24,94
1 273	7 519	627	27,66
1 373	7 492	646	29,01
1 473	7 444	666	30,37
1 573	7 396	687	31,74
1 627	7 368	699	32,44
1 645	7 350	706	32,45
1 659	7 332	712	32,32
1 668	7 317	716	32,15
1 675	7 301	721	31,91
1 683	7 273	729	31,43
1 693	7 222	743	30,39
1 701	7 153	763	28,87
1 873	6 987	823	27,58

M. Copur and M. N. Eruslu, Metallurgical and Materials Engineering Department, Istanbul Technical University, Maslak Istanbul, Turkey
A. Turan, Yalova Community College, Yalova University, Yalova, Turkey

Table 2 Thermo-physical properties of green sand [8]

T /K	Green Sand - Machine Molded		
	ρ kg/m ³	C_p J/kg K	k W/m K
295	1 404	0	0,000
373	1 392	953	0,548
473	1 380	994	0,535
573	1 367	1 035	0,511
673	1 363	1 076	0,484
773	1 358	1 117	0,452
873	1 352	1 158	0,418
973	1 348	1 198	0,386
1 073	1 345	1 239	0,360
1 173	1 342	1 280	0,347
1 273	1 339	1 321	0,347
1 373	1 335	1 362	0,369
1 473	1 332	1 403	0,417
1 573	1 329	1 444	0,497
1 673	1 326	1 485	0,618
1 773	1 323	1 526	0,783
1 873	1 320	1 567	1,001

METHODOLOGY

Two sizes of chills were used to analyze the effects of the chill size on the solidification pattern and the feeding distance. The segmented volume of the small

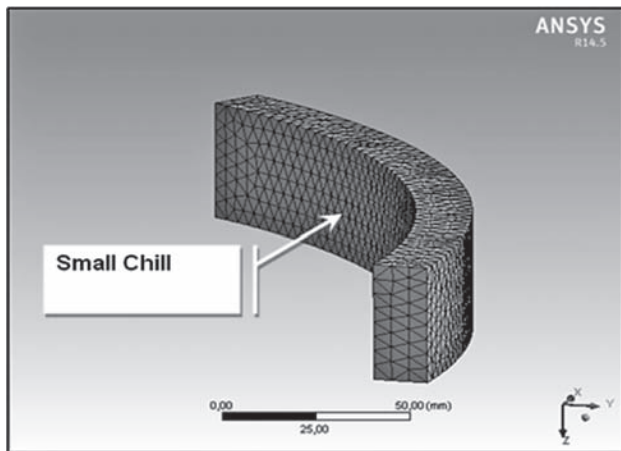


Figure 1 3D model of the small chill

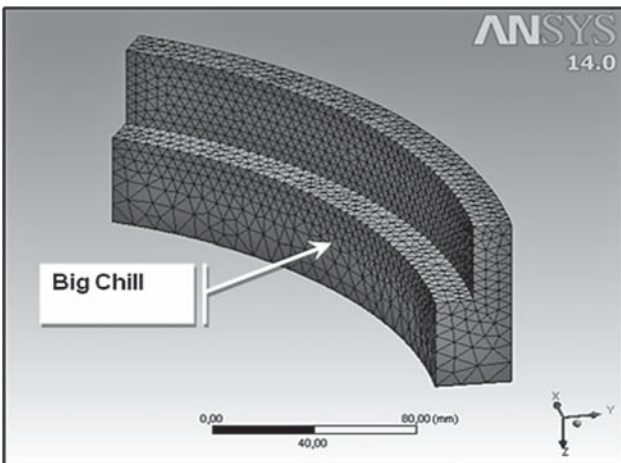


Figure 2 3D model of the big chill

chill is 122 cm³ (Figure 1), and the segmented volume of the big chill is 393 cm³ (Figure 2).

TRANSIENT ANALYSES

In this study, the geometry of the model was segmented as 6 pieces of 60° symmetric parts.

Liquidus and solidus temperature of AISI 1016 steel are 1 790 K and 1 750 K respectively.

As the initial conditions, at t = 0 s, 1 973 K was assigned to impeller (metal) as it was 298 K for the chills, the core and the mold. The convection created by the natural aerated environment have film coefficient values 5,75 W/(m²K) and 11,45 W/(m²K) for the mold top/bottom surfaces and outer vertical surface respectively [10-14]. Side surfaces of the segmented model are set as adiabatic as the initial boundary condition.

RESULT AND DISCUSSION

The aim of this study is to understand the effects of the chills on the solidification pattern and their contributions on the feeding distance.

In Figure 3, it is seen that the liquid metal (red zones) passage between outer shell of the impeller and the riser gets narrower at t = 65 s as the outer shell still needs liquid metal to solidify without shrinkage.

In the analysis, it is well understood that the solidification on the outer shell is incomplete when the connection between outer shell and the riser is broken.

Figure 4 shows the small chill application in contact to the outer shell. The solidification of the outer shell is separated into two locations by small chill. The lower part of the outer shell solidifies without supply of liquid metal from riser.

As it is seen in Figure 4, small chill makes the solidification pattern worse. Thus, there is a minimum size of a chill to have sufficient and proper impact on the solidification pattern.

A model with bigger chill was analyzed (Figure 5). Solidification on the outer shell occurs only on a single location at t = 30 s as it was seen in the model of small chill. The solidification rate on the outer shell is faster

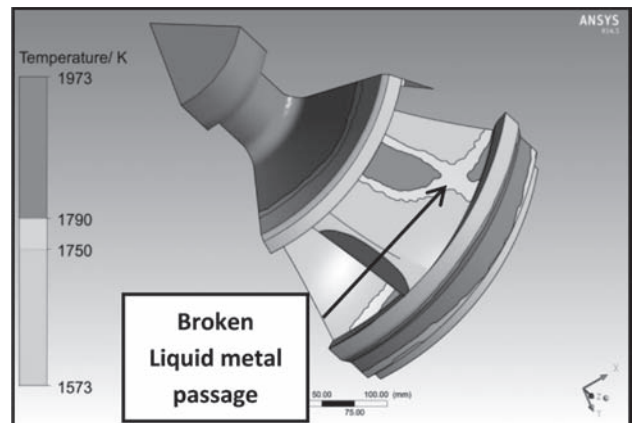


Figure 3 Impeller without chill at t = 65 s

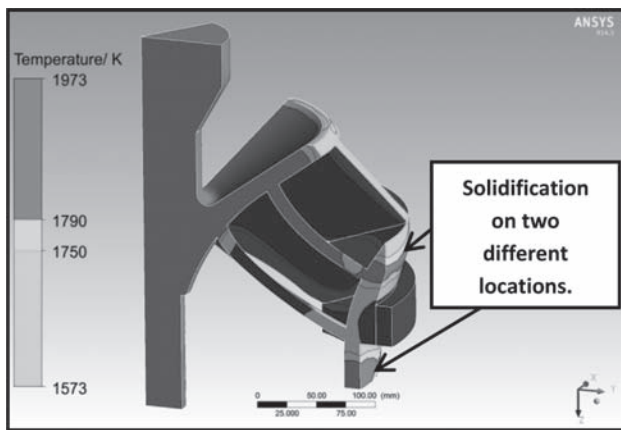


Figure 4 Impeller, core, small chill at $t = 35$ s

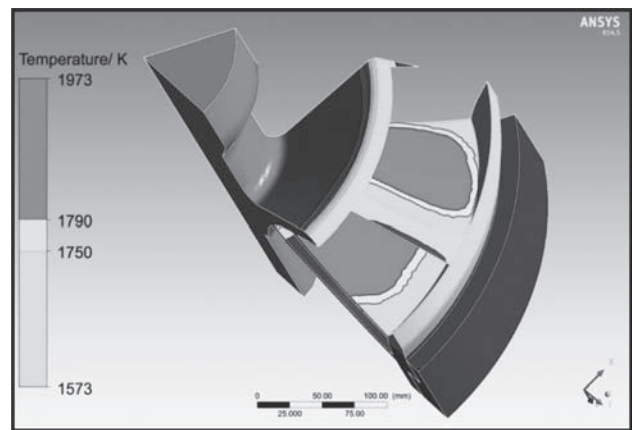


Figure 7 Impeller and big chill at $t = 45$ s

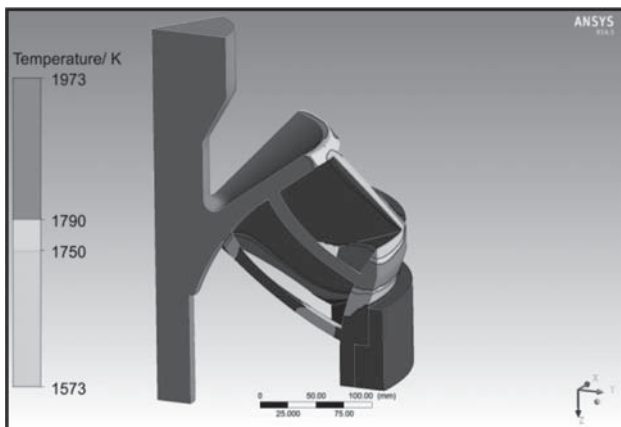


Figure 5 Impeller, core, big chill at $t = 30$ s

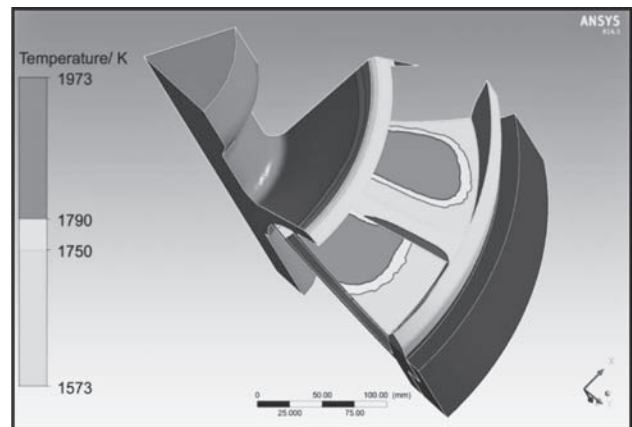


Figure 8 Impeller and big chill at $t = 50$ s

in the model of big chill. Thus, outer shell becomes solid as the feeding path from the riser is still liquid.

At the solidification steps of $t = 42,5$ s, 45 s and 50 s, the solidification contours are seen in the Figure 6, Figure 7 and Figure 8 respectively.

As it is seen in FIGURE 6-8, the solidification contour draws back in the direction of the riser. In every step, the feeding path is not disconnected and the liquid metal is supplied to the locations that solidify. We can conclude that the big chill provides the directional solidification in the impeller casting.

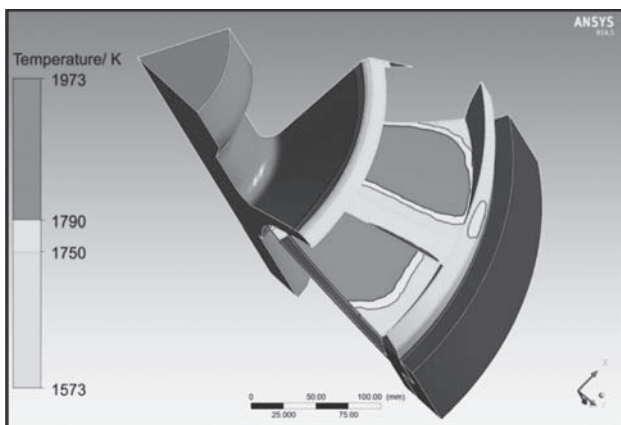


Figure 6 Impeller and big chill at $t = 42,5$ s

CONCLUSION

In this study, transient heat transfer equations were solved to estimate the effect of the chill and their sizes on the solidification pattern of an impeller by using Ansys CFX.

Unfortunately, there is no quantitative data or a formula to calculate the feeding distance of a riser in a given riser-metal-chill-core-mold combination. How feeding distances of risers can be increased in a complex geometry by using chill, chill size and their locations should be analyzed for each case (geometry) by using numerical methods. So, each model which consists of cast part (including riser), core, mold and chills should be studied separately.

The model with no chill showed that the directional solidification was impossible to create. The small chill did not contribute the directional solidification, but rather made the solidification pattern worse and raised the possibility of shrinkage on the outer shell. The model with big chill is the only one which created directional solidification.

REFERENCES

- [1] R. D. Pehlke, A. Jeyarajan and H. Wada: Michigan Univ., Report No. NSFMEA82028, 1982.
- [2] K. Harste: PhD Dissertation Thesis, 1989, Technical University of Claustal.

- [3] J. Miettinen, *Metall. Trans. B*, 28B (1997), 281-297.
- [4] M. J. Keil, J. Rodriguez and S. N. Ramrattan: *AFS Transactions*, 107 (1999), 71-74.
- [5] C. A. Santos, J. M. V. Quaresma and A. Garcia, *Journal Alloys and Compounds*, 319 (2001) 174-186.
- [6] S. I. Bakhtiyarov, R. A. Overfelt and D. Wang, *International Journal of Thermophysics*, 26 (2005), 141-149.
- [7] A. C. Midea and M. Burns, *International Foundry Research*, 59 (2007), 34-43.
- [8] M. J. Peet, H. S. Hassan and K. D. H. Bhadeshia, *International Journal of Heat and Mass Transfer*, 54 (2011), 2602-2608.
- [9] R. W. Lewis, K. Morgan, H. R. Thomas and K. N. Seetharamu, *The Finite Element Method in Heat Transfer Analysis*, Wiley, Wiley, New York, 1996.
- [10] M. J. Keil, J. Rodriguez and S. N. Ramrattan: *AFS Transactions*, 107 (1999), 71-74.
- [11] M. M. Pariona and A. C. Mossi: *J. Of rge Braz. Soc. Of Mech. Sci. And Eng.*, 27 (2005), 399-406.
- [12] *ANSYS Thermal Analysis Guide*, Ansys Inc., Canonsbyrg, 2010, USA.
- [13] *ANSYS Handbook*, Chapter 6, Ansys Inc., Canonsbyrg, USA. 2011.
- [14] M. Copur, M.N.Eruslu, *Metalurgija*, 53 (2014) 2, 149-15

Note: The responsible for English language is Lecturer from Istanbul Technical University, Turkey